Proceedings of the International Conference on Industrial Engineering and Operations Management

Publisher: IEOM Society International, USA DOI: 10.46254/NA10.20250065
Published: June 17, 2025

Tracking the Unseen: Autonomous Multi-Object Motion Analysis in Complex Environments

V. Ann Schrimpsher, Hieu Pham, Ana Wooley and Anyama Tettey
University of Alabama in Huntsville
Huntsville, AL 35899, USA

Sampson Gholston
University of Texas at Arlington, Arlington
TX 76019, USA
vas0001@uah.edu

Abstract

In typical object detection and tracking methods, separating the image background clutter from the object of interest is a challenging but necessary task. The more dynamic the background clutter, the more difficult the desired object is to trace. In this paper, instead of separating the unwanted sections of an image from the object, we decided to use the dynamic background clutter to help detect the presence of an object and to track its periodic motion. With the use of digital signal processing in combination with partial fast Fourier transformation (pFFT), an algorithmic process called Periodic Motion Detection (PMD) is used to autonomously detect an object by plotting the fluctuations that occur within a background when an object comes into the field-of-view (FOV). These changes are then converted into a digital signal format and fed into a pFFT to determine the frequency in which the object appears. The detection of an object becomes apparent when a pattern emerges in the random background fluctuation signal and when the level of change within that signal reaches a specific threshold. Experimental results show that photometric disturbances, which are a type of dynamic background clutter, can be used to autonomously detect multiple objects and predict the frequency of the appearances of those objects.

Keywords

Multi-object tracking, Autonomous detection, Periodic motion detection, Data mining, Dynamic background clutter.

1. Introduction

Computer Vision Detection (CVD) in manufacturing is credited with reducing production costs (Micali et al. 2016) and human error (Qeshmy et al. 2019), while increasing efficiency (Feng et al. 2019). CVD can be used to detect anything from wildfires to defects on printed circuit boards (Wang et al. 2016) to handwashing procedures. Many of the objects or events that are monitored through CVD occur with reliable intermittent periodicity. Some of these events include products on an assembly line, heartbeats (He et al. 2019), orbiting satellites, traffic workflow patterns, daily migratory patterns of animals (Liu, et al. 2016), employee/robotic motion patterns, and movements associated with Parkinson's disease (Pereira, et al. 2016). Discovering an event and determining its periodicity can help management implement a plan to improve the situation by uncovering inefficiencies within the system. Unfortunately, detecting and tracking these types of objects or events can be difficult for many reasons. Three main reasons for this difficulty are 1) the recording manner involved with monitoring these types of objects is usually discontinuous, 2) dynamic background clutter (DBC) exists in the targeted object's environment creating noise, and 3) when multiple objects appear in the same timeframe, the detection signal loses its pattern. By focusing on object detection and tracking, this paper will address these three reasons by interpreting their nature and explaining how they can be overcome.

The experiment performed in this study used data collected by NASA's Kepler Space Telescope monitoring astronomical events and consisted of two scenarios where the motion of three objects with long-term periodicity was captured on a charged-coupled device (CCD) camera while they moved in front of a single light source. The first scenario monitored only one object. After a process, i.e. the Periodic Motion Detection (PMD) process, was developed and verified that it had the ability to recognize a single targeted object and determine that object's period, a second scenario was observed where two targeted objects with overlapping trajectories were monitored to see if the PMD process could be adapted to perceive the two objects separately and ascertain their corresponding periods.

The PMD process was able to detect and track all three objects in both scenarios through a modular approach. The first step was to convert the digital discontinuous images into data points, creating a discrete digital signal. That discrete digital signal went through additional processing until the signal was modified into a continuous waveform. The next step involved separating the object indicators from the noise. Noise, in this case, is connected to the DBC. Typically, DBC is separated from an object of interest before recognition verification of that object occurs. This study took a different approach. Instead of focusing on removing the DBC, the newly processed digital signal was normalized so that threshold values that can distinguish the fluctuations in the DBC caused by noise from the fluctuations caused by the appearance of an object could be uncovered. The final step was to take the normalized data and put it through a partial fast Fourier transformation (pFFT) process. This pFFT translated the digital signal from cartesian coordinates into polar coordinates. The local minimums found in the polar coordinates were used to verify the existence of the objects and calculate their periodicity.

1.1 A Subsection Sample

The objectives of this research are as follows:

- To address three primary challenges in object detection and tracking: discontinuous data recording, DBC, and multiple object detection with overlapping trajectories.
- To develop and validate the PMD process as an alternative approach for handling DBC and improving object detection accuracy.
- To demonstrate the PMD process's effectiveness in tracking both single and multiple objects, including those with overlapping trajectories, and calculating their periodicity.
- To apply digital signal processing and pFFT to convert discrete signals into continuous waveforms and identify object periodicity.
- To present a modular approach to object detection, integrating data normalization, noise separation, and signal transformation.

2. Background Review

Using DBC as a periodic-motion object detection tool is a novel idea. However, the detection techniques described in this paper that are used to track objects with periodic motion have been developed over time. Both static and moving cameras have been used to track and classify objects in real time since 1999. From the images of these cameras, an object's periodicity and self-similarity characteristics were used in detection and classification. Time-frequency analysis was applied to follow the object's evolution over time (Cutler and Davis 1999).

By 2005, the self-similarity metric was no longer needed to detect specific objects and determine their periodicity. Oscillations in intensity values that are induced at specific time instances along linear sample paths were used instead. The location of the peaks of intensity was used to create a full-intensity profile. Sample paths were obtained by connecting sample points from regions of high motion magnitude (Thangali and Sclaroff 2005).

The next year, the self-similarity metric was added back into the process by plotting the trajectories of the features, called feature power vectors, associated with the self-similarity metric over time. An optical motion capture system used these trajectories to make motion templates. To classify an object, these templates were then compared to pre-stored motion templates to seek out the best motion power spectral similarity (Meng et al. 2006).

In 2014, the focus changed to being able to detect objects in dynamic cluttered environments and various types of occlusions. All background images were classified as noise and removed completely from the object of interest's silhouette. Occlusions such as object-object occlusions and object-scene occlusions were dealt with by contour tracking of the targeted object's outline (Kumar et al. 2014).

Discrete periodic events, where an object's motion occurs at specific time intervals instead of continuously, that occurred in the presence of noise was the basis of research in 2017. A model was developed that created discrete periodic motion associated with an object and incorporated false-positive events as well as, the possibility that the underlying period and phase of the events would change over time. Sequential Monte Carlo methods were employed to filter out the targeted object's motion and eliminate the noise (Ghosh et al. 2017).

In 2018, a multi-object tracking application was created using a multi-Bernoulli filter to detect each object while removing unwanted image clutter. This method was evaluated using real-world scenarios and video (Kim, 2018). Later that year, an FFT using autocorrelation and cross-correlation was implemented to detect similar features within two images. This method creates a response map whose values represent the probability of each pixel in an image belonging to the target (He et al. 2018).

Recent work has shown that biologically-inspired vision systems can significantly enhance object detection in cluttered or low-contrast environments by mimicking adaptive filtering mechanisms found in insect visual systems (Uzair et al. 2020). Similarly, cross-disciplinary approaches—such as the use of phylogenetic and geostatistical models for autonomous robot guidance—demonstrate the effectiveness of signal-driven algorithms in target detection (Schrimpsher and Gholston 2019). In 2021, a novel optical camera architecture called FourierCam was introduced, using programmable frequency-domain sampling to directly measure the pixel-wise temporal spectrum of a video. This approach allowed for real-time machine vision tasks such as background subtraction, object-extraction, and trajectory tracking, while reducing detection bandwidth and computational load (Hu et al. 2021).

While using DBC as a detection tool has not been studied directly, the groundwork for research into this area has been done. The insights gained into filters and image classification can be used as a guide to a new level of detection design. This application of DBC monitoring makes this investigation the next logical step in the object detection process.

2.1 Periodic Motion Detection (PMD) Process Methodology

This process was designed to detect multiple objects with long-term levels of periodicity through the observation of photometric disturbances generated by the objects themselves. Through this same information, the time interval corresponding to each object will also be determined. The data in the surveillance input files is expected to be discrete, broken, and missing bits of information. From this fragmented data, the PMD process will remove the noise and create a continuous stream of data to use as inputs into the detection procedure. For this experiment, the time units of any data will be rescaled to minutes.

2.2 Digital Signal Processing (DSP)

To detect an object with periodicity and determine its frequency of occurrence that object must be monitored over long periods of time. Seldom is this type of monitoring continuous. Images are normally captured seconds, minutes, and sometimes hours apart. This creates images that are disconnected. That disconnection in conjunction with the targeted object appearing periodically means some details of the object's behavior may not be recorded. The missing information is compensated for via the digital signal processing (DSP) technique called exponential interpolation

The input files used in the PMD process included a list of the highest intensity values found in each image. Each image is time-stamped. Plotting the intensity values versus time in a 2D graph made it possible to create a time-series plot that showed the photometric disturbances that are generated by either the noise inherent in the light source or the appearance of the targeted objects. Unfortunately, at this point, the graph shows a series of sporadic data points, see **Figure** 1(a). To transcribe the data into a continuous waveform, the data points had to be smoothed.

2.3 Exponential Interpolation

To start the smoothing process, an exponential interpolation method was used to find consistent, evenly spaced time-series intensity readings. Interpolated intensity readings were spaced 0.01-time units apart. When plotted, the raw data was not a straight line. Therefore, the exponential interpolation function in Equation (1) was used because it assumes a smooth, concave curved pattern between points (Linear and non-Linear Interpolation 2018). Once the files have been interpolated, the data points can be concatenated producing a continuous digital signal like the one in **Figure** 1(b).

$$fc=[fa](b-c)(b-a)*[fb](c-a)(b-a) \quad (1)$$

Where, a = time at initial intensity value
b = time at final intensity value
c = desired time, this is the time you want an intensity value for
$f(a)$ = intensity at point a
$f(b)$ = intensity at point b
$f(c)$ = interpolated intensity at point c.

2.4 Dynamic Background Clutter (DBC)

When a system is attempting to identify a target, objects are differentiated by tracing an outline that separates it from any background clutter based on a signature, such as color. Background clutter is when the area around an object of interest produces significant signatures that make it difficult to distinguish the target from the background. When the background is continuously changing, due to fluctuations or movement, for instance, it makes this process even more difficult. This type of clutter is called Dynamic Background Clutter (DBC). Another difficulty in tracking an object is if the object's motion causes it to momentarily leave the sensor's field-of-view (FOV). Not only does the system have to separate the target object from its background, but it also must determine when the object is in the FOV. However, just as DBC affects the object's signal to the sensor, the object affects the DBC's signature. If the object moves with a near-regular period, it is possible to use the changes seen in the DBC signature by the sensor to infer where the target is.

The DBC that was the focus of this study was oscillating photometric intensity levels. The presumption was that negative fluctuations in intensity would be greatest when an object moved into the FOV. If the target object appeared in the FOV at regular intervals, then the periodicity of that object could be determined as well. Unfortunately, noise inherent within the system was interwoven with the periodic events. This noise presented itself with the same amplitude or greater than the signal we were trying to detect and created fluctuations that were uncorrelated with any periodic signal. To subdue the effects of the noise, the normal fluctuations that occur in the DBC had to be understood. This understanding was used to develop thresholds that would show which fluctuations were anomalies and which were innate to the system.

Flicker and Pulsation.

As with all sources of light, noise is present in the form of flickering and pulsating. Flickering is minor changes in intensity that have low amplitudes and very high frequencies. Flickering depends on the fuel source and the nature of the system. Flickering, which can be seen in. Figure. 1(a), means the intensity values will not appear in a straight line. An intensity measurement will always be either a little higher or a little lower than the previous measurement.

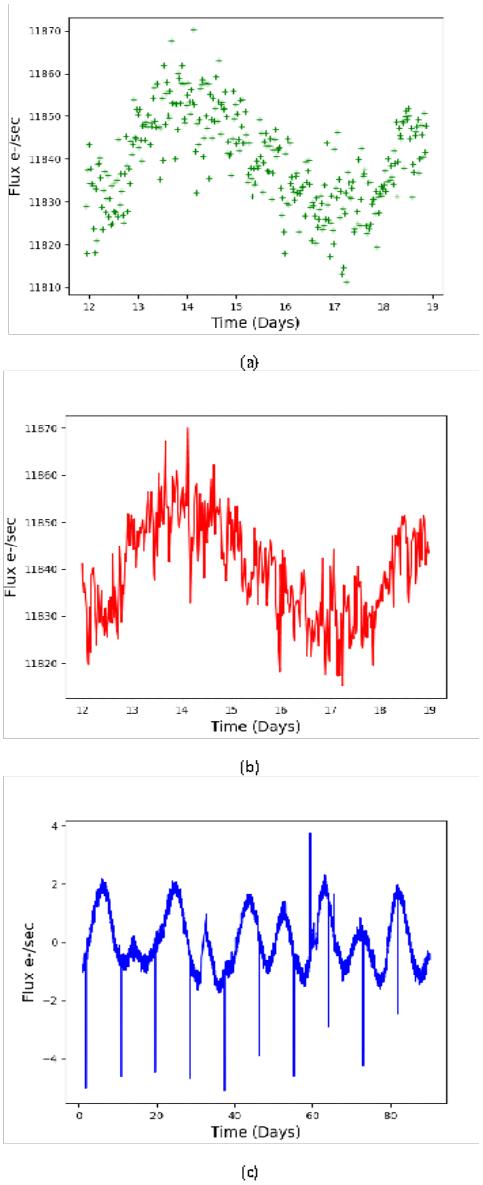

Figure 1. Transformation of the Input Data as it goes from initial raw data (a), to smoothed data (b), and finally to normalized data (c).

Pulsating is major changes in intensity that have high amplitudes and low frequencies. The level of pulsating varies from light source to light source and depends on variations within the system and environmental factors. The effects of pulsating can be seen best when measurements are taken over longer periods of time as in **Figure**. 1(c). Pulsating makes intensity measurements appear to pulsate in a sinusoidal wave pattern.

2.6 Normalization

Normalization of the data was implemented to remove much of the noise and to help find intensity measurement outliers. Outliers represent the possible detection of an object of interest. The mean and standard deviation (SD) of the initial raw data was found to help facilitate these processes and to help find thresholds that differentiated which intensity measurements were noise due to flicker and which were outliers. By calculating the mean, a center point from which the SD is set was established. In the data seen in **Figure** 1(a), the SD was found to be 46.35255. This means that any point more than 3 SDs away from the center point will be an outlier. The 3-sigma limit was used because it is a good balance point between the two major types of statistical errors (Montgomery 2013).

Next, the interpolated data, seen in Figure. 1(b), was normalized by setting the mean equal to zero and the SD equal to one by using (2). Normalization had to be done because the intensity values are so large and the noise due to pulsation causes so much variation that the range of values for intensity was too great to work with efficiently. The mean and SD values used in (2) were the values calculated from the initial raw data. Figure. 1(c) is a graph of the normalized data. Notice that the values on the y-axis have changed immensely as compared to Figure. 1(a) and Figure. 1(b).

$$z_{t_i} = \frac{x_{t_i} - \mu}{\sigma} \quad (2)$$

Where, μ = the mean of the initial raw data
σ = the standard deviation of the initial raw data
x_{t_i} = the intensity value at time equal to t_i
z_{t_i} = the new normalized intensity value at time equal to t_i
i = 1 , 2, 3, . . .

3. Dynamic Background Clutter (DBC)

Fourier Transforms (FT) take a signal and express it in terms of the frequencies of the waves that make up that signal. This is very important if your signal is threaded with noise or if the signal will not appear in a perfect lock-step pattern because of multiple objects appearing in the same timeframe. FTs are very versatile. They can take on the form of a single dimension of space and can be expanded up to multiple dimensions. A Fast Fourier Transform (FFT) differs from a traditional Fourier Transformation in that it windows the signal and transforms each segment into the frequency domain. A partial Fast Fourier Transform (pFFT) simplifies the FFT by using fewer dimensions of space than are available for analysis. The PMD process uses a pFFT**.**

To understand how pFFT is applied to this problem, a few terms must be defined. Correlation is the process of establishing a relationship between two or more measures in a series of data. Two types of correlation are used in this process, cross-correlation and autocorrelation. Cross-correlation matches measurements across multiple sets of time-series data. Autocorrelation correlates measurements within a single signal over different time delays. Windowing is the process of partitioning a dataset into subsections, which increases the dimension shape of the dataset so that those sections can be compared. In essence, windowing divides a single time series data set into multiple data sets. These multiple datasets can then be cross-correlated.

To track an object with periodic motion, the system needs to identify it multiple times over the course of the time-series data. This is done in a few steps. First, the data is windowed into partitions based on a chosen frequency. Next, each window is cross-correlated with all subsequent windows to scan for the existence of similar measurements within the chosen frequency. This process is repeated for multiple frequencies until either an object is found, or the list of viable frequencies is exhausted. The frequency of which an object is detected is an estimate of that said object's period. To complete this process, the final step is to verify the object's existence and increase the precision of the estimated period through autocorrelation. Before any correlation can be performed, the time-series data must be transformed into the frequency domain.

Once the data in this experiment was normalized, the signal could be fed into the pFFT part of the PMD process. The pFFT produced the polar graph seen in Fig. 2(a). The purpose of the pFFT is to convert the time associated with the signal into a number of different candidate frequencies. Each frequency is a guess at the object's period, where "x" frequencies represent the "x" number of time units per rotation. For example, if the frequency equaled 7 Hertz, then there would be 7 seconds of the signal plotted per rotation on the polar graph. Since it was known that the targeted objects had periods in the range of 1 to 10 minutes, the frequency values were incremented by 0.1 from 1 minute to 10 minutes. Each rotation for each frequency was searched for outliers. Any outliers that were found below the central mean line were transferred to an Outlier Table (OT).

Even though the data had been normalized, when plotted on the polar graph, the signal still fluctuated drastically. This fluctuation can be seen in **Figure** 2(a). The pFFT data was normalized again in segments and called Segmented Normalized Data (SND). The rotations of the SND overlapped within the polar graph like the one seen in **Figure** 2(b). This made searching for outliers and comparing the angles associated with the outliers in one rotation to

subsequent rotations possible. This process for creating the SND polar graph, capturing and recording any outliers, and finding the object by angle comparison required the use of the algorithms seen in **Figure** 3.

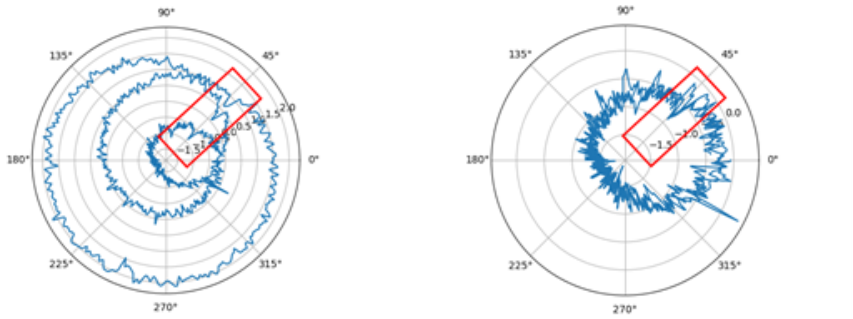

Figure 2. Transformation of the polarized data as it changes from the original transformation (a) to segmented normalized data (b). The red box on both graphs indicates a detected object of interest. There are three rotations in both graphs. The frequency of this graph is 5.9 cycles per minute.

Algorithm 1:
Algorithm 1 is the Normalization Algorithm seen in **Figure** 3(a). This algorithm transforms the signal generated by the pFFT seen in **Fig**. 3(a) into the segmented normalized version of that signal seen in **Figure** 2(b). Once the data is in this form, the Outlier Table (OT) mentioned previously is created. The definitions of the variables are as follows: φ is the width of a segment, f = frequency, τ is the threshold SD value to determine if an intensity measurement is classified as an outlier, T is the set of times, I is the set of intensities, t is the current time, i is the intensity measurement, θ is the set of angles within all the rotations, r is the new intensity value after normalization, s is the segment, μ_s is the mean of the intensity values within a segment, μ_{base_s} is the mean of the intensity values of the current segment within the first rotation, δ_i is the offset between the segment mean of the first rotation and segment means in all other rotations. Restrictions on variables include the following: $\varphi, f, and\ \tau$ have to be greater than zero, T and I cannot equal zero. For all t that are an element in the set of times, there is an ordered pair (t, i) ,and t and i in this ordered pair are elements in the set of times and the set of intensities. For all ordered pair (t, i) that are elements in the set of times and the set of intensities, the ordered pair (t, i) will be mapped to the ordered pair (θ, r) such that θ equals Equation 3 and r equals the normalized value of i for each φ.

$$\theta = \frac{2\pi t}{f_{target}} \tag{3}$$

Where, t = time
f_{target} = current rotation

Explanation of Algorithm 1: For each segment of element θ with width φ, the $\mu_s$is equal to the mean of all the intensity values within that segment. If **s** is less than 360°, then δ_i equals zero and μ_{base_s} equals μ_s. Otherwise, δ_i equals the mean of the current rotation segment minus the mean of the corresponding segment in the first rotation. For every ordered pair (**t**, **i**) that are elements in the set of times and the set of intensities set θ equals (3). Set **r** equal to the intensity value minus the offset. Set **Δr** equal to the mean of the segment in the first rotation minus the current value of **r**. If **Δr** is greater than τ, then r at the current theta is an outlier. **Note**: all outliers are possible targets.

Algorithm 1 PFFT

Require: $\phi > 0, f > 0, \tau > 0, T \neq \emptyset, I \neq \emptyset, \forall t \in T \; \exists (t,i) \in (T,I)$

Ensure: $\forall (t,i) \in (T,I). (t,i) \rightarrow (\theta, r) \; s.t. \; \theta = \frac{2\pi t}{f_{target}}, r = Norm(i, \phi)$

1: **for** *each* $s \in \Theta$ *width* ϕ **do**
2: $\mu_s \Leftarrow mean(i \in s)$
3: **if** $s < 2\pi$ **then**
4: $\delta_i \Leftarrow 0$
5: $\mu_{s_{base}} \Leftarrow \mu_s$
6: **else**
7: $\delta_i \Leftarrow \mu_s - \mu_{s_{base}}$
8: **end if**
9: **end for**
10: **for** *each* $(t,i) \in (T,I)$ **do**
11: $\theta \Leftarrow \frac{2\pi t}{f}$
12: $r \Leftarrow i - \delta_i$
13: $\Delta r \Leftarrow \mu_{s_{base}} - r$
14: **if** $\Delta r > \tau$ **then**
15: $outliers \Leftarrow \{(\theta, r), (t, i)\}$
16: **end if**
17: **end for**

(a)

Algorithm 2 Object Finder

Require: Rotations, $\rho > 0, Outliers, O \neq \emptyset$

Ensure: Find period of candiate objects

1: $\Theta_{2\pi} \Leftarrow \{\forall O[\theta] : 0 \leq \theta < 2\pi\}$
2: $\Theta_{after2\pi} \Leftarrow \{\forall O[\theta] : \theta \geq 2\pi\}$
3: **for** *each basecandiate* $\in \Theta_{2\pi}$ **do**
4: **for** *each candiate* $\in \Theta_{after2\pi}$ **do**
5: **if** $relativeangle(candiate[\theta]) = basecandiate[\theta] \pm \varepsilon$ **then**
6: $C \Leftarrow candiate$
7: **end if**
8: **end for**
9: **if** $|C| \geq \rho - 1$ **then**
10: $period \Leftarrow averageDistance(C[time])$
11: **end if**
12: **end for**

(b)

Figure 3. These are the two algorithms used in the PMD process: (a) is the algorithm used to generate the outlier table and (b) is used to generate the minimum table.

Algorithm 2: Algorithm 2, seen in **Figure**. 3(b), is the Local Minimum Angle Algorithm. This algorithm takes every nominal angle associated with a local minimum within a polar graph's first rotation and compares it to all other nominal angles associated with a local minimum within all subsequent rotations in the same polar graph. The output of this algorithm is a list of objects of interest and their associated time periods. The definitions of the variables are as follows: ρ is the number of rotations, O is the set of outliers, $\theta_{2\pi}$ is all the angles less than 360°, $\theta_{after2\pi}$ is all the angles greater than 360°, ε is the threshold angle error value that accounts for phase shift, C is the possible object of interest and all associated metrics. Restriction on variables include the following: ρ has to be greater than zero. O cannot equal zero.

Explanation of Algorithm 2: $\theta_{2\pi}$ equals a list of local minimum angles found in the first rotation. $\theta_{after2\pi}$ equals a list of local minimum angles found in all subsequent rotations. For each possible object of interest's angle within the first rotation check to see if this angle equals any other angle that is found in the other rotations within a predefined margin of error. Store this list of angles in the variable C. If the number of matching angles is at least equal to ρ minus 1, then calculate the period of the object of interest by subtracting the distance between each angle, then taking the average of those distances.

From the OT, the data was processed to create **Table** 1, the Minimum Table (MT). The OT was searched for local minimums. Every local minimum with its corresponding metrics was transferred over to the MT. Once the MT was complete, every value in the table was evaluated by comparing each value's nominal angle in the first rotation to every value's nominal angle in every other rotation via the Local Minimum Angle Algorithm, see **Fig**. 3(b). For example, if there is a local minimum at 315° in the first rotation, then all successive rotations are assessed to see if there is a local minimum at 315° within them. If an angle match is found in n-2 rotations, where n equals the total number of rotations, then it is hypothesized that an object of interest has been found. When an object of interest has been discovered, the period of that object is calculated by taking the average difference of the times between each occurrence of the object.

Table 1. A sample of the Minimum Table is shown below. This is the table generated where an object is found on the normalized polar graph at approximately 315 degrees (highlighted). The calculated time interval between each object-appearance is 5.9123 minutes.

rotation	intensity	angle	normalized_angle	time
5.9123	-0.85665	42.014106	42.0141	0.72
5.9123	-1.09440	65.15231	65.1523	1.1
5.9123	-1.59343	105.33972	105.3397	1.76
5.9123	-1.11230	281.92074	281.9207	4.66
5.9123	-0.89257	315.41025	315.4102	5.21
5.9123	-1.39141	429.88346	69.8835	7.09
5.9123	-0.84274	646.6519	286.6519	10.65
5.9123	-0.82905	675.2702	315.2702	11.12
5.9123	-0.55877	702.0618	342.0618	11.56
5.9123	-0.77196	723.37331	3.3733	11.91
5.9123	-1.40591	770.86751	50.8675	12.69
5.9123	-1.84724	830.53972	110.5397	13.67
5.9123	-1.77375	895.08313	175.0831	14.73
5.9123	-1.43509	941.35954	221.3595	15.49
5.9123	-1.28443	957.19094	237.1909	15.75
5.9123	-1.08224	983.98254	263.9825	16.19
5.9123	-0.58222	1035.7391	315.7391	17.04
5.9123	-0.51930	1070.4464	350.4464	17.61
5.9123	-0.77267	1091.7579	11.7579	17.96
5.9123	-1.14199	1115.505	35.5050	18.35
5.9123	-1.45954	1136.8165	56.8165	18.7
5.9123	-1.27219	1295.7394	215.7394	21.31
5.9123	-0.50647	1395.599	315.5990	22.95

5.9123	-1.72372	1512.5078	72.5078	24.87
5.9123	-1.75395	1534.4282	94.4282	25.23
5.9123	-0.52237	1754.8501	314.8501	28.85
5.9123	-0.79609	1796.8642	356.8642	29.54

Because the initial measurements acquired of the event occurrences were not a continuous stream of images, matching local minimums can appear to be slightly out of phase, see Figure. 4. This graph shows two signals with the same amplitude and same frequency, but slightly out of phase with each other.. This means in one rotation, the object of interest's nominal angle may be 315.8°, while in another rotation, the object of interest's nominal angle may be 314.5°. A threshold of a 4° angle difference was determined through trial-and-error to allow for a difference in apparent phase without getting false-positive nominal angle readings.

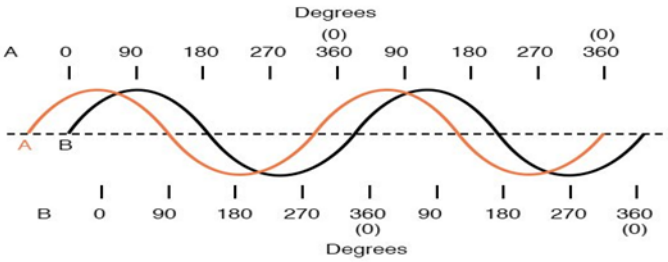

Figure 4. This graph shows two signals with the same amplitude and same frequency, but slightly out of phase with each other.

4. Data Collection and Experimental Setup

The PMD process was constructed in the Python programming language using the equations, algorithms, and thresholds discussed in this paper. The data used in this experiment is from the NASA Archive, where NASA was observing an astronomical event by monitoring changes in the background photometric intensity while objects of interest with periodicity came within the sensor's FOV. The sensor was a CCD camera located on the Kepler Space Telescope. Data from two specific events were used. One event included the effects produced by one object. The second event included the effects produced by two objects with overlapping trajectories. The original input data can be found in the files kplr000757076-2010274085026_llc.fits (scenario one) and kplr006959607-2010265121752_llc.fits (scenario two) at the NASA website.

These scenarios were used to test the PMD process' ability to detect and track objects and calculate their respective periodicity. In each case, the images from the CCD camera were converted into discrete digital signals, which were then processed using DSP techniques. The pFFT was applied to the processed signal to determine the frequency of each object's appearance in the FOV. Data was stored as digital image files and signal outputs that were later analyzed using the custom software described in this document to validate the periodicity calculations.

4.1 Periodic Motion Detection (PMD) Process Results and Analysis

The results of this study demonstrated that the PMD process is effective in detecting and tracking objects with periodic motion, by using the fluctuations in the DBC caused by the objects of interest. By capturing these fluctuations via camera and applying a modular approach in processing and analysis of the image data, the PMD process successfully determined the periodicity of each object autonomously.

Table 2. The mean, standard deviation (SD), and %error associated with each object.

Comparison of Experimental Results to Actual Results					
Scenario One					
	Raw Data		Actual Period	Experimental Period	%Error
	Mean	SD			
Object 1	11861.387	43.59	8.8849212844	8.8857142857	8.93*10-3
Scenario Two					
	Raw Data		Actual Period	Experimental Period	%Error
	Mean	SD			
Object 1	15187.500	46.35	5.91227219	5.9114285714	1.43*10-2
Object 2	15187.500	46.35	8.98584700	8.9871428571	1.44*10-2

To verify the validity of the process, the periodicity estimates must closely approximate the known periodicity of the three objects in the two studied scenarios. As shown in **Table** 2, the experimental period exhibited a %error of approximately 10-2 percent.

It is important to note the several benefits of autonomous detection. First, it enables efficiency by allowing for continuous, 24/7 data collection without the need for human intervention, significantly reducing both time and resource demands. It also ensures scalability, as it can handle large datasets from multiple sources simultaneously, making it ideal for complex, large-scale environments. Furthermore, accuracy is enhanced as autonomous systems track and analyze data with greater precision, minimizing the potential for human error. Additionally, autonomous detection reduces costs by eliminating the need for constant human labor and facilitating operations in hazardous environments where human presence might be unsafe. Lastly, it supports long-term monitoring, maintaining continuous data collection over extended periods and making it crucial for tracking slow or rare events, such as seasonal trends or health patterns.

5. Conclusion

Using Computer Vision Detection (CVD) an object with discrete periodic motion, such as an employee moving back and forth between two pieces of equipment to complete a job, can be detected and its periodicity can be determined. Once this information has been calculated, inefficiencies within the manufacturing process can be uncovered and removed. This study wanted to determine if a process could be developed to detect objects with periodic motion and overlapping trajectories using the disturbances in dynamic background clutter (DBC) created by the targeted objects themselves. It also wanted to see if this process could calculate the frequency in which the objects appeared within a sensor's FOV. This was a challenge since typically the dynamic background clutter is seen as an obstacle to object detection and is removed early in the object detection task. In a technique called the PMD process, a modular approach designed to handle discontinuous data combined digital signal processing and pFFT to convert discrete signals into continuous waveforms and autonomously identify objects periodicity. The PMD process was tested on two scenarios. The first scenario contained one object. It was able to detect this single object and find its period within a %error of 8.93*10-3. The second scenario included two objects, whose trajectories overlapped. It was able to detect both objects separately and determine their periods within a %error of 1.4*10-2.

Even though this method is able to determine an object's periodicity with very high accuracy and precision, it does have limitations. It is specifically designed for detecting objects that exhibit periodic motion, and is not well-suited for identifying non-repeating or irregular movement patterns. Additionally, accurate detection relies on a sufficiently long observation window to capture full motion cycles; shorter sequences or partial periods may reduce the reliability of the results. In a separate study currently under review, the PMD algorithm was benchmarked against 11 machine learning models. The results showed that PMD performed either equivalently or better in terms of accuracy, precision, recall, and specificity, while also being computationally faster by an order of magnitude. Unlike the machine learning models, PMD's data mining–based design also offers greater transparency, making it well-suited for applications where explainability is critical (Schrimpsher et al. in press). This benchmarking study provides further evidence of the PMD method's practical value and complements the contributions presented in this paper. In the future, this process will be tested to see if it can detect several objects with overlapping trajectories and whose periods range from very small to very large. It is our hope that the combination of pFFT with the normalization process can enhance the CVD

system so that true outliers associated with everything from product measurements to human behavior can be uncovered and the outlier's cause can be eliminated.

Disclosure of Interests

The authors have no competing interests

References

Cutler, R., & Davis, L. Real-time periodic motion detection, analysis, and applications. *Proceedings from the 1999 IEE Computer Society Conferernce on Computer Vision and Pattern Recognition*, 2, 326-332, 1999.

Feng, X., Jiang, Y., Yang, X., Wu, M., & Li, X. Computer vision algorithms and hardware implementations: A survey. *Integration*, vol. 69, pp. 309-320, 2019.

Ghosh, L., Lucas, C., & Sarkar, R. Finding periodic discrete events in noise streams. *Proceedings from the 2017 ACM on Conference on Information and Knowledge Management*, pp. 627-636, 2017.

He, Z., Niu, J., Ren, J., Shi, Y., & Zhang, W. A deep learning method for heartbeat detection in ECG image. *Chinese intelligent automation conference,* pp. 356-363, 2019.

He, Z., Zhang, Z., & Jung, C. Fast Fourier transform networks for object tracking based on correlation filter. *IEEE Access*, vol. 6, pp. 6594-6601, 2018.

Hu, C., Huang, H., Chen, M., Yang, S., & Chen, H. FourierCam: a camera for video spectrum acquisition in a single shot. *Photonics Research*, *9*(5), 701-713, 2021.

Kim, D. Visual multiple-object tracking for unknown clutter rate. *IET Computer Vision*, vol. 12, no. 5, pp. 728-734, 2018.

Kumar, P., Chakraborty, R., & Sarkar, A. Robust object tracking under cluttered environment. *International Journal of Emergency Technology and Advanced Engineering,* vol. 1, pp. 18-19, 2014.

Linear and Non-Linear Interpolation. *Mr. Math,* Retrieved from https://www.mrmath.com/misfit/algebra-stuff/linear-and-non-linear-interpolation/ on May 13, 2022, 2018.

Liu, T., Chen, W., Wu, W., Sun, C., Guo, W., & Zhu, X. Detection of aphids in wheat fields using a computer vision technique. *Biosystems Engineering*, vol. 141, pp. 82-93, 2016.

Meng, Q., Li, B., & Holstein, H. Recognition of human periodic movements from unstructured information using a motion-based frequency domain approach. *Image and Vision Computing* vol. 24, no. 8, pp. 795-809, 2006.

Micali, M., Cashdollar, H., Gima, Z., & Westwood, M. One touch workpiece verification system for cnc maching using a low-cost computer vision approach. *International Manufacturing Science and Engineering Conference,* pp. 3, 2016.

Montgomery, D. *Introduction to Statistical Quality Control 7th Edition*, pp. 245, 2013.

Pereira, C., Pereira D., Silva, F., Masieiro, J., Weber, S., Hook, C., & Papa, J. A new computer vision-based approach to aid the diagnosis of Parkinson's disease. *Computer Methods and Programs in Biomedicine*, vol. 136, pp. 79-88, 2016.

Qeshmy, D., Makdisi, J., da Silva, E., & Angelis, J. Managing Human Errors: Augmented Reality systems as a tool in the quality journey. *Procedia Manufacturing,* vol. 28, pp. 24-30, 2019.

Schrimpsher, V., & Gholston, S. Phylogenetic-Kriging Technique Reduces Search-Time of Autonomous Unmanned Vehicles in Simulation. In *IIE Annual Conference. Proceedings* (pp. 366-371). Institute of Industrial and Systems Engineers (IISE), (2019)

Schrimpsher, V., Gholston, S., & Morris, A. A Micro-Services Modular Based Architecture to Reduce Rigidity, Complexity, and Noise in Human Computer Interaction Systems. In *IIE Annual Conference. Proceedings* (pp. 1624-1629). Institute of Industrial and Systems Engineers (IISE), 2018

Schrimpsher, V., Gholston, S., Pham, H., Wooley, A. and Tettey, A., Bridging the Black Box: Data Mining Enhanced Machine Learning Interpretability for Exoplanet Discovery, *Proceeding of the 10th North American Conference on industrial Engineering and Operations Management (IEOM),* Orlando, Florida, in press.

Thangali, A., & Sclaroff, S. Periodic motion detection and estimation via space-time sampling. *Proceedings from the 2005 Seventh IEEE Workshops on Applications of Computer Vision*, vol. 1, pp. 176-182, 2005.

Uzair, M., Brinkworth, R. S., & Finn, A. Bio-inspired video enhancement for small moving target detection. *IEEE Transactions on Image Processing*, *30*, 1232-1244, 2020.

Wang, L., Yang, Z., Zhou, Y., & Hao, J. Calculation of flexible printed circuit boards (FPC) global and local defect detection based on computer vision. *Circuit World*, vol. 42, no. 2, 2016.